Oxygen Abstraction from Dioxygen on the Al(111) Surface

Andrew J. Komrowski, Jonathan Z. Sexton, and Andrew C. Kummel
U.C.S.D. Department of Chemistry and Biochemistry, La Jolla, California 92093

Marcello Binetti, Olaf Weiße, and Eckart Hasselbrink
Fachbereich Chemie, Universität Essen, 45117 Essen, Germany
(Received 4 June 2001; published 26 November 2001)

Abstractive chemisorption in the initial oxidation of Al(111) has been experimentally verified using variable incident energy O_2. Scanning tunneling microscopy images show a transition between single O-adatom reaction products to more pairs of O-adatom reaction products as the O_2 incident energy is raised from 0.025 to 0.8 eV. The ejected O atoms have been detected in the gas phase with resonant enhanced multiphoton ionization. The observations that both abstractive and dissociative chemisorption are activated processes are in contrast to current adiabatic models of the absorption process.

DOI: 10.1103/PhysRevLett.87.246103 PACS numbers: 68.35.Ja, 68.37.Ef

Understanding the initial stages of the oxidation of the Al(111) surface remains a challenge in gas-surface dynamics. Experimentally, Österlund *et al.* reported that dissociative adsorption is a direct, activated process starting with only 1% reaction probability for thermal (0.025 eV) molecules but rising to 90% reaction probability at an incident energy E_i of 0.9 eV [1]. However, several computational studies predict near unity reaction probability even at low E_i, since the calculated potential energy surfaces (PES) exhibit no barrier to dissociation for most impact parameters and molecular orientations [2,3]. This discrepancy can be interpreted either as a manifestation of the present accuracy obtainable in generalized-gradient approximation (GGA) calculations, or as an indication of the significance of nonadiabatic effects [4]. The GGA PES suffer from the calculated LUMO on O_2 being degenerate with the Fermi level in Al(111); this artificially facilitates barrierless resonant electron transfer from Al(111) to O_2.

In this Letter, we present compelling evidence that at low translational energies the sticking of O_2 to a pristine Al(111) surface is dominated by an abstraction mechanism, whereby one atom from O_2 chemisorbs on the surface while the other atom is ejected back into the gas phase. Scanning tunneling microscopy (STM) of samples exposed to a monoenergetic O_2 beam confirm the high percentage of single O-adatom reaction products. Laser spectroscopy detects the O atoms escaping from the surface into the gas phase.

The results presented here are suited to resolve the apparent contradictions which arose following the original interpretation of the preeminent STM investigation upon the initial oxidation of Al(111) by Brune *et al.* who identified the initial reaction products of thermal O_2 with Al(111) as single chemisorbed oxygen adatoms [5]. In contrast, pairs of adatoms are commonly imaged with STM as the normal result of dissociative chemisorption of diatomics on close-packed transition metal surfaces [6]. Brune *et al.* proposed that hot adatom motion of more than 80 Å following O_2 bond fission was responsible for the observed random adatom distribution reasoning that hot adatom motion may be enabled by the high exothermicity of the dissociation process [5]. Modeling by Wahnström *et al.* [7] showed that the direction of motion will be rapidly randomized such that the final O-atom separation will not exceed 20 Å. As an alternative, abstractive chemisorption ($O_{2(g)} + Al_{(s)}$-O-$Al_{(s)} + O_{(g)}$) has been proposed [8]. Since the binding energy of a single O atom to the Al(111) surface (7.5 eV) is larger than the bond energy of O_2 (5.12 eV), abstraction is thermodynamically allowed [9].

The results of the O_2/Al(111) STM experiments were obtained in an UHV-STM chamber equipped with a differentially pumped molecular beam [10]. An aluminum single crystal (Monocrystals Company) was cleaned by sputtering with Ar^+ ions created with a differentially pumped ion gun (VG Microtech). During the sputter cycles (2 hours, 2 kV ion energy, 10-A filament emission), the sample was radiatively heated from the backside to a surface temperature of 550 ± 20 °C. The room temperature surface was dosed at normal incidence with an O_2 molecular beam seeded in an inert gas in order to vary the translational energy.

The molecular beam scattering experiments have been performed in a similar apparatus [11]. A molecular beam is derived from a pulsed nozzle, skimmed, and chopped such that gas pulses of ~100 μs length and a peak flux of 10^{15} molecules $cm^{-2}\,s^{-1}$ result. The molecular beam strikes the Al(111) sample at 45° with a cross section of 4 mm. In the scattered flux of O_2 molecules, O atoms are detected by (2 + 1)-photon resonant multiphoton ionization (REMPI) at 226 nm. A frequency doubled, tunable dye laser producing 2.5 mJ/pulse, is focused by a 250 mm lens with the focus located 10 mm away from the sample in the direction of the surface normal. Because of this geometrical arrangement, the experiment is largely insensitive to the angular distribution of the O atoms released from the surface reaction. O atoms are ionized

through a resonant transition from the $(2p)^3P_2$ ground state to the $(3p)^3P_{0,1,2}$ state as intermediate.

It is widely observed that oxygen atoms on metal surfaces are detected as depressions in STM constant-current images [5,6,9,12–18]. Figure 1 shows a high-resolution STM images of the Al(111) surface reacted with oxygen. Three dark sites in the image are assigned to be single chemisorbed oxygen atoms (S), and one site is assigned as two chemisorbed oxygen atoms at adjacent sites ($P \equiv$ paired site; approximately twice the area of a single O-adatom site). This assignment scheme is consistent with what was employed in the original STM study of the O-Al(111) system [5]. The small apexes in the middle of the depressions, shown in lines 1 and 3, have previously been assigned as due to oxygen adatoms [5]. Experimentally, it is seen that changing the tunneling conditions or tip morphology can increase the height of the oxygen apex. Interestingly, the position of the oxygen apex is neither directly at a threefold hollow site nor at an a-top site. However, STM images have conclusively shown that the oxygen apexes within larger islands of chemisorbed oxygen reside at fcc threefold hollow sites [12]. It is likely that the low coverage intermediate position of the single chemisorbed oxygen apex is due to a local substrate lattice rearrangement [3,19] and/or due to asymmetric electronic orbital interference in the tip-adsorbate interaction. The difference in appearance between the line 1 and line 2 sites may be due to occupation of nearly degenerate adsorption sites on the Al(111) surface (similar to other metals, see [13,15]). Calculations show that there are four chemisorption sites of O atoms on Al(111) with binding energies within $\pm 5\%$ [20]; this would easily explain the existence of multiple adsorption sites.

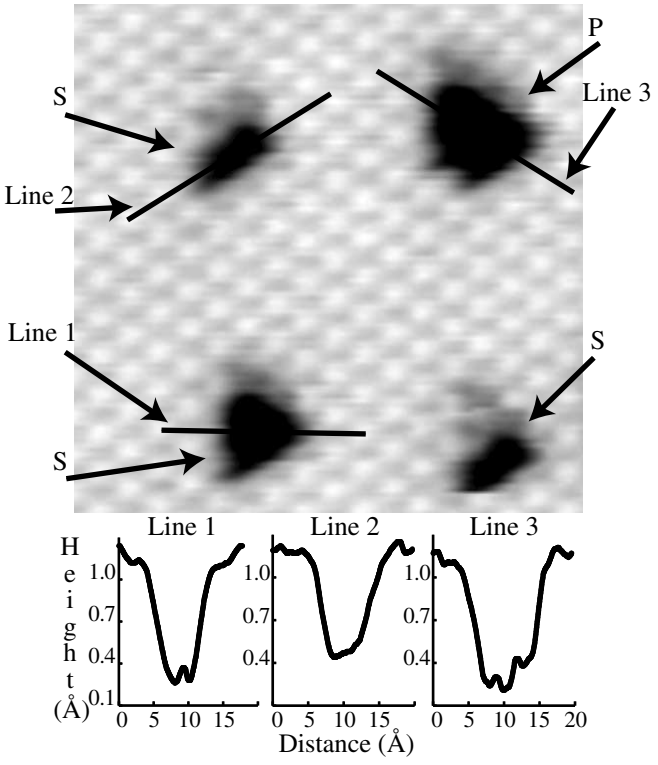

FIG. 1. High resolution STM image of chemisorbed oxygen features on the Al(111) surface, tunneling conditions: $I_{\text{tunnel}} = 70$ nA, $V_{\text{sample}} = -0.8$ V. Image size 45 Å $\times$ 45 Å. Scan direction: fast, left to right; slow, top to bottom. Three line traces are drawn through O-Al reacted sites and plotted: line 1, a single oxygen adatom site; line 2, a slightly different single adatom site; line 3, a paired site. Reacted sites are labeled as single O-adatom sites (S), or paired sites (P).

It should be noted that the above interpretation of STM images has recently been debated. The imaging of small O-Al(111) reacted sites has been perceived by Schmid *et al.* as consisting of clusters of two or three adatoms on the room temperature surface [21]. While it is not possible for us to completely disprove this claim, there is significant evidence to support the original interpretation of Brune *et al.* [5]. First, the imaging of 1×1 chemisorbed oxygen islands is in agreement with previous LEED studies [22] and has been tied to low coverage STM results in recent experiments [12]. The 1×1 islands can be observed at coverages below 5% monolayer (ML) and have the identical structure to the islands at 1 ML coverage. Second, the size and shape of the O-Al(111) sites first identified by Brune *et al.* as single O adatoms is in agreement with the assignment of chemisorbed oxygen adatoms on the Ag(111) [14], Ag(001) [13], Ru(0001) [18], and Pt(111) [6,15] surfaces. Third, theoretical simulation of O-Al(111) STM images have reinforced this assignment [9]. Fourth, our data shows that as the translation energy of O_2 is increased, the island density decreases while the ratio of double to single sites increases. This is inconsistent with surface diffusion as the cause of the site distribution because diffusion is independent of incident translation energy. Fifth, some of the single sites appear elongated along one of the threefold symmetric axes, and Schmid *et al.* interpreted this as proof these sites consisted of two atoms. However, in real time STM movies we observed that these elongated sites can convert to triangle sites and back to elongated sites. This is inconsistent with the elongated sites being composed of two atoms but is consistent with our assignment of these features as single oxygen atoms with an STM shape influenced by a local surface relaxation, metastable bonding, or tip-surface interaction.

STM images were analyzed for evidence of long-range pairwise O-adatom chemisorption at separate sites. If a hot-adatom or cannonball mechanism were active in the adsorption process, two O adatoms would be expected to appear simultaneously in an STM image. No such correlation of O-adatom chemisorption events was detected.

Figures 2a and 2b show typical STM images of surfaces dosed with 0.11 and 0.8 eV O_2 molecules, respectively. The surface substrate atoms are not visible in these images, but the adsorbate features are resolved. Each reacted site

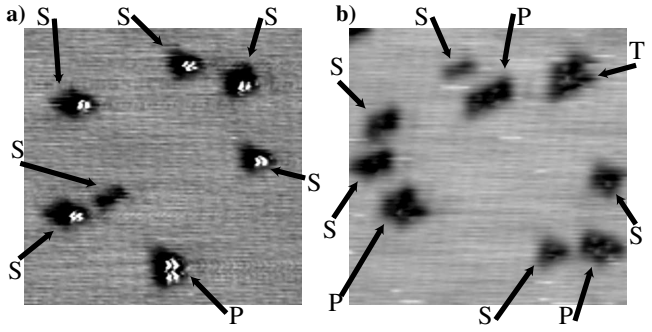

FIG. 2. STM images of Al(111) surfaces reacted with monoenergetic molecular beams of O_2. Reacted sites are labeled as single O-adatom sites (S), paired sites (P), or trimers (T). Image sizes 52 Å × 52 Å, scan directions: fast, left to right; slow, bottom to top. (A) 0.11 eV O_2 beam; tunneling conditions: $I_{\text{tunnel}} = 15$ nA, $V_{\text{sample}} = -0.1$ V. (B) 0.8 eV O_2 beam; tunneling conditions: $I_{\text{tunnel}} = 30$ nA, $V_{\text{sample}} = -0.1$ V.

in Fig. 2 is identified as a single oxygen atom (S), a pair of oxygen atoms chemisorbed at adjacent sites (P), or as a small island of three oxygen atoms (T). Surfaces dosed with high translational energy O_2 contain more paired oxygen adatoms than surfaces dosed with low translational energy O_2. We propose that the isolated single sites are due to abstractive chemisorption while the paired sites result from dissociative chemisorption. The three-adatom sites are due to coincidental consecutive adsorption events at adjacent surface positions. Enhanced reactivity near preexisting O adatoms has been modeled [23] to successfully reproduce island growth.

Figure 3 plots the results of the adsorbate size distribution analysis as the ratio of single chemisorbed oxygen atoms to oxygen pairs (S/P) versus O_2 incident energy. At an O_2 incident energy of 0.8 eV, 60% of the oxygen features are adsorbed as single adatoms, and 30% are adatom pairs—corresponding to $S/P = 2$. This result may be contrasted with the data from the thermal O_2 dosed surface, $S/P = 15$.

Using REMPI, the oxygen atom yield has been recorded for three different translational energies of the incoming molecules. Under our experimental conditions, the yield of O ions is about 0.1 per laser pulse. Using REMPI time of flight spectrometry, we have convinced ourselves that the observed signals do not arise from photodissociation of scattered or background O_2 molecules or from impurities contained in the molecular beam [16]. The primary data has been corrected for the variation in flux of the incoming beam due to the dilution by the seeding gas. Further, it has been assumed that the O atoms resulting from the abstraction reaction have a velocity distribution that does not vary with the translational energy of the incoming O_2 molecule—as has been experimentally verified. Therefore, the corrected flux of O atoms is directly proportional to the yield of abstracted atoms per incoming molecule (Fig. 4). Unfortunately REMPI does not allow for an absolute calibration of the observed flux. However, we estimate that the observed signal corresponds to a partial sticking coefficient for abstraction between 10^{-3} and 0.1. The REMPI partial sticking coefficient for abstraction is small because the REMPI experiment measures abstraction events relative to incident flux while STM results reported here measure the abstraction to dissociation ratio.

The data show a marked increase of the abstraction probability with translational energy. Time-of-arrival measurements indicate a 0.35 eV translational energy for the ejected O atoms.

Together, the STM and REMPI experiments can be reconciled only if one assumes that an abstraction mechanism is operative. However, the STM and REMPI experiments probe different aspects of the variation of the sticking coefficient, S, with translational energy of the incoming molecules. The STM experiments give evidence that the total sticking coefficient is composed of two partial coefficients, namely one for the abstraction process,

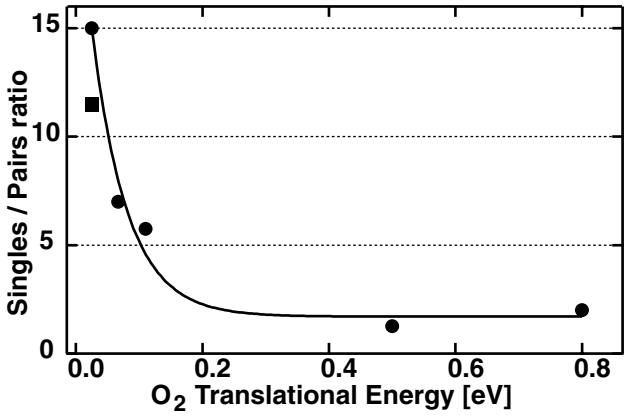

FIG. 3. Adsorbate distribution analysis from STM data. The ratio of single chemisorbed oxygen adatoms to oxygen pairs (S/P) versus O_2 incident energy. (●) Present study; (■) Brune *et al.* thermal O_2 study [5]. The line is drawn to guide the eye. The absolute oxygen coverage is 0.005–0.037 ML.

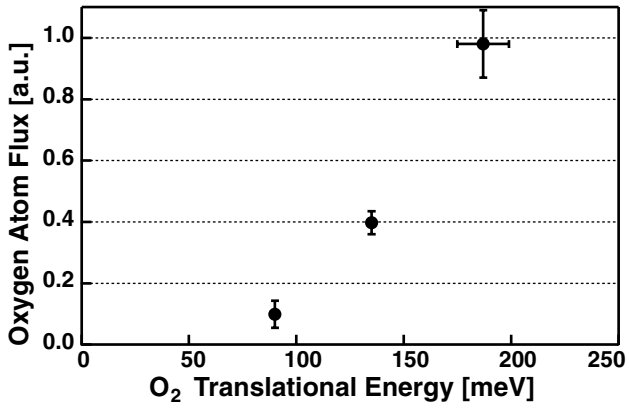

FIG. 4. O-atom yield per incoming O_2 molecule as a function of translation energy of the incoming molecule.

S_a, and one for ordinary dissociative chemisorption, S_d. The singles to pairs ratio recorded in STM experiments provides the ratio of these two partial coefficients, S_a/S_d. the REMPI measurement probes the absolute change of S_a with increasing energy . Since S_a increases with energy and the S_a/S_d ratio decreases with energy, it follows that S_d increases more rapidly with energy than S_a. Hence, we conclude that at low energies abstractive chemisorption dominates while at high energies both processes contribute with nearly equal weight.

We have shown that a doubly bonded diatomic molecule that requires the transfer of two electrons to break its internal bond undergoes abstraction on a close-packed metal surface. From a dynamical point of view, it is interesting to consider why an atom is ejected rather than forms a bond to the surface. In studies of reactions on low work function metal surfaces, it has been theoretically predicted [24] and experimentally shown [25] that abstractive chemisorption is favored for collisions with the incident molecule oriented end-on. Recently, Yourdshahyan *et al.* have calculated the adiabatic O_2 + Al(111) potential energy surface for different molecular orientations while concurrently allowing the charge on the molecule to freely change along the reaction coordinate [3]. They predict that charge transfer to form O_2^- occurs prior to significant lengthening of the internal O_2 bond and at a greater gas-surface distance for end-on collisions. From this argument, it follows naturally that an abstraction channel may exist. In the end-on geometry, the outer O atom is too far away from the surface to form a bond when the second charge transfer occurs. On the other hand, charge transfer is too inefficient in the side-on geometry at low translational energies to account for a significant sticking coefficient. Therefore, at low incident translation energy, only end-on oriented O_2 react with Al(111) and the chemisorption is abstractive because this orientation is favorable for both charge transfer and abstraction.

Our experimental results show that increased translational energy activates both abstraction and dissociation reactions. Conversely, the adiabatic O_2/Al(111) density functional theory (DFT) potentials calculated by state-of-the-art spin-polarized GGA methods [2,3] show no barrier to reaction in the entrance channel. This difference likely indicates the dominance of nonadiabatic effects in the O_2/Al(111) reaction which are *a priori* excluded in the GGA DFT calculations. In a simplified model, delayed charge transfer along $O_2 \rightarrow O_2^- \rightarrow O_2^{-2}$ would be an origin of nonadiabaticity giving rise to a reaction barrier in the entrance channel. This view is backed by an extension of the diabatic Norskov-Newns-Lundqvist model used for modeling nonadiabatic reaction of Cl_2/K [26] that is able to account for the observed activated sticking of O_2/Al(111) [27]. However, nonadiabatic effects in the exit channel are probably negligible because the experimental and adiabatic theoretical results agree that abstractive chemisorption is a common event.

M. B. thanks the CEC for support through the TMR program (ERB FMRX-CT98-0249). The STM experiment was funded by NSF Grant No. CHE-0074813. We thank Dr. Andreas Eichler for useful discussions.

[1] L. Österlund, I. Zoric, and B. Kasemo, Phys. Rev. B **55**, 15 452 (1997).
[2] K. Honkala and K. Laasonen, Phys. Rev. Lett. **84**, 705 (2000); T. Sasaki and T. Ohno, Surf. Sci. **433–435**, 172 (1999).
[3] Y. Yourdshahyan, B. Razaznejad, and B. I. Lundqvist, Solid State Commun. **117**, 531 (2001).
[4] M. Brandt *et al.,* Phys. Rev. Lett. **81**, 2376 (1998); T. Greber, Curr. Opin. Solid State Mater. Sci. **3**, 446 (1998); T. Greber, Appl. Phys. A **67**, 701 (1998); T. Greber, Surf. Sci. Rep **28**, 1 (1997); G. Katz, Y. Zeiri, and R. Kosloff, Surf. Sci **425**, 1 (1999).
[5] H. Brune *et al.,* Phys. Rev. Lett. **68**, 624 (1992); H. Brune *et al.,* J. Chem. Phys. **99**, 2128 (1993).
[6] J. Wintterlin, R. Schuster, and G. Ertl, Phys. Rev. Lett. **77**, 123 (1996).
[7] G. Wahnström, A. B. Lee, and J. Strömquist, J. Chem. Phys. **105**, 326 (1996); C. Engdahl and G. Wahnström, Surf. Sci. **312**, 429 (1994).
[8] K. A. Pettus, P. R. Taylor, and A. C. Kummel, Faraday Discuss. **117**, 321 (2000); L. E. Carter *et al.,* J. Chem. Phys. **100**, 2277 (1994); J. A. Jensen, C. Yan, and A. C. Kummel, Science **267**, 493 (1995); Y. Liu, D. P. Masson, and A. C. Kummel, Science **276**, 1681 (1997).
[9] J. Jacobsen *et al.,* Phys. Rev. B **52**, 14 954 (1995).
[10] C. Yan, J. A. Jensen, and A. C. Kummel, J. Chem. Phys. **102**, 3381 (1995).
[11] A. de Meijere, E. Kolasinski, and E. Hasselbrink, Faraday Discuss. Chem. Soc. **96**, 265 (1993).
[12] J. Trost *et al.,* J. Chem. Phys. **108**, 1740 (1998).
[13] S. Schintke *et al.,* J. Chem. Phys. **114**, 4206 (2001).
[14] C. I. Carlisle *et al.,* Surf. Sci. **470**, 15 (2000).
[15] B. C. Stipe *et al.,* Phys. Rev. Lett. **78**, 4410 (1997); B. C. Stipe, M. A. Rezaei, and W. Ho, J. Chem. Phys. **107**, 6443 (1997).
[16] M. Binetti *et al.,* Faraday Discuss. **117**, 313 (2000).
[17] T. Zambelli *et al.,* Nature (London) **390**, 495 (1997).
[18] J. Wintterlin *et al.,* Surf. Sci. **394**, 159 (1997).
[19] G. Henkelman and H. Jónsson, Phys. Rev. Lett. **86**, 664 (2001).
[20] A. Kiejna and B. I. Lundqvist, Phys. Rev. B **63**, 085405 (2001).
[21] M. Schmid *et al.,* Surf. Sci. Lett. **478**, L355 (2001).
[22] S. A. Flodström *et al.,* Phys. Rev. Lett. **40**, 907 (1978).
[23] M. L. Neuburger and D. P. Pullman, J. Chem. Phys. **113**, 1249 (2000).
[24] J. Strömquist *et al.,* Surf. Sci. **352–354**, 435 (1996).
[25] M. Brandt *et al.,* Surf. Sci. **404**, 160 (1998); M. Brandt *et al.,* Surf. Sci. **439**, 49 (1999).
[26] J. K. Norskov, D. M. Newns, and B. I. Lundqvist, Surf. Sci. **80**, 179 (1979); L. Hellberg *et al.,* Phys. Rev. Lett. **74**, 4742 (1995).
[27] A. Hellman *et al.* (to be published).